

Article

Phospholipid Hydrolysis Caused by *Clostridium perfringens* α -toxin Facilitates the Targeting of Perfringolysin O to Membrane Bilayers

Paul C Moe, and Alejandro P Heuck

Biochemistry, Just Accepted Manuscript • Publication Date (Web): 01 October 2010

Downloaded from <http://pubs.acs.org> on October 1, 2010

Just Accepted

“Just Accepted” manuscripts have been peer-reviewed and accepted for publication. They are posted online prior to technical editing, formatting for publication and author proofing. The American Chemical Society provides “Just Accepted” as a free service to the research community to expedite the dissemination of scientific material as soon as possible after acceptance. “Just Accepted” manuscripts appear in full in PDF format accompanied by an HTML abstract. “Just Accepted” manuscripts have been fully peer reviewed, but should not be considered the official version of record. They are accessible to all readers and citable by the Digital Object Identifier (DOI®). “Just Accepted” is an optional service offered to authors. Therefore, the “Just Accepted” Web site may not include all articles that will be published in the journal. After a manuscript is technically edited and formatted, it will be removed from the “Just Accepted” Web site and published as an ASAP article. Note that technical editing may introduce minor changes to the manuscript text and/or graphics which could affect content, and all legal disclaimers and ethical guidelines that apply to the journal pertain. ACS cannot be held responsible for errors or consequences arising from the use of information contained in these “Just Accepted” manuscripts.



1
2
3
4
5 **Phospholipid Hydrolysis Caused by *Clostridium perfringens* α -Toxin**
6 **Facilitates the Targeting of Perfringolysin O to Membrane Bilayers[†]**
7
8

9
10 Paul C. Moe and Alejandro P. Heuck[‡]
11

12
13 Department of Biochemistry and Molecular Biology, University of Massachusetts, Amherst,
14 MA 01003, USA.
15
16

17
18
19
20 Running title: Alpha-toxin activity facilitates PFO cytolysis
21
22
23

24
25 [‡]Corresponding Author:

26 Dr. Alejandro P. Heuck
27 710 N. Pleasant St.
28 Lederle GRT Rm 816
29 University of Massachusetts
30 Amherst, MA 01003
31 Phone: (413) 545-2497, Fax: (413) 545-3291
32 Email: heuck@biochem.umass.edu
33
34
35

36 [†] This work was supported in part by an award from the American Heart Association to A.P.H..
37
38
39
40
41
42
43
44
45
46
47
48
49
50
51
52
53
54
55
56
57
58
59
60

1
2
3
4
5 1 **Abbreviations:** PFO, perfringolysin O; CDCs, cholesterol-dependent cytolysins; LLO,
6
7 listeriolysin O; POPC, 1-palmitoyl-2-oleoyl-*sn*-glycero-3-phosphocholine; POPE, 1-palmitoyl-2-
8
9 oleoyl-*sn*-glycero-3-phosphoethanolamine; DAG, 1-palmitoyl-2-oleoyl-*sn*-glycerol; GSH,
10
11 reduced L-glutathione; OG, Oregon Green-488X; Fl, fluorescein; PC, phosphatidylcholine; PI,
12
13 phosphatidylinositol; SM sphingomyelin; DTT, (2*S*,3*S*)-1,4-bis-sulfanylbutane-2,3-diol; EDTA,
14
15 ethylenedinitrilotetraacetic acid; D4, domain 4; DPA, dipicolinic acid.
16
17
18
19
20
21
22
23
24
25
26
27
28
29
30
31
32
33
34
35
36
37
38
39
40
41
42
43
44
45
46
47
48
49
50
51
52
53
54
55
56
57
58
59
60

ABSTRACT

Clostridium perfringens causes gas gangrene and gastrointestinal disease in humans. These pathologies are mediated by potent extracellular protein toxins, particularly α -toxin and perfringolysin O (PFO). While α -toxin hydrolyzes phosphatidylcholine and sphingomyelin, PFO forms large transmembrane pores on cholesterol-containing membranes. It has been suggested that the ability of PFO to perforate the membrane of target cells is dictated by how much free-cholesterol molecules are present. Given that *C. perfringens* α -toxin cleaves the phosphocholine head group of phosphatidylcholine, we reasoned that α -toxin may increase the number of free-cholesterol molecules in the membrane. Our present studies reveal that α -toxin action on membrane bilayers facilitates the PFO-cholesterol interaction as evidenced by a reduction in the amount of cholesterol required in the membrane for PFO binding and pore-formation. These studies suggest a mechanism for the concerted action of α -toxin and PFO during *C. perfringens* pathogenesis.

1
2
3
4
5
6
7
8
9
10
11
12
13
14
15
16
17
18
19
20
21
22
23
24
25
26
27
Clostridial myonecrosis or gas gangrene, a fulminant human infection inflicted by several Gram-positive *Clostridium* species, promotes a painful and fast destruction of healthy tissue if not properly treated with antibiotics. *Clostridium perfringens* type A is the most common bacterium isolated from patients presenting trauma-induced gas gangrene. Analysis of infected tissues shows edema, thrombosis, and restriction of leukocyte infiltration to the perivascular regions in the infected site. This complex pathology is mediated by potent extracellular protein toxins, especially α -toxin (a phospholipase C) and θ -toxin (perfringolysin O or PFO) (1). While α -toxin hydrolyzes phosphatidylcholine (PC) and sphingomyelin (SM), PFO forms large transmembrane pores on cholesterol-containing membranes. Of the several exotoxins produced by *C. perfringens*, only α -toxin and PFO have been implicated in pathogenesis (2).

28
29
30
31
32
33
34
35
36
37
 α -Toxin is essential for growth and spread of infection in the host (3) and it helps *C. perfringens* avoid the host defense mechanism by altering the normal traffic of the host phagocytes (4, 5). The role played by α -toxin in pathogenesis is dictated by its ability to interact with membranes, whether from outside the cell or while inside the phagosomes (6).

38
39
40
41
42
43
44
45
46
47
48
49
50
51
52
53
54
55
56
57
58
59
60
PFO is the prototypic member of the cholesterol-dependent cytolysin (CDC) family that includes listeriolysin O (LLO), streptolysin O (SLO), pneumolysin, and others (7-9). The CDC are β -barrel pore-forming toxins that are secreted by the bacterium as monomeric water-soluble proteins (10). Upon encountering a cholesterol containing membrane (11-14), PFO monomers bind (15, 16), oligomerize and form ring-like structures (17, 18), that ultimately insert a large β -barrel into the membrane (19-22). Despite the progress made in understanding the molecular mechanism of PFO cytolysis (14, 15, 23, 24), the importance of PFO in the development and progression of *C. perfringens* gas gangrene is less well understood. Interestingly, it has been

1
2
3 shown that PFO and α -toxin exhibit a synergic effect in the establishment of the infection and
4
5 development of gangrene (1, 3, 25).
6
7

8 We have shown that PFO binding to model membranes requires a relatively high
9
10 concentration of cholesterol (16, 26), and the ability of PFO to puncture the membrane seems to
11
12 be dictated by how much free cholesterol is present in the lipid bilayer (11, 27-30). Similar
13
14 effects were observed for the activity of cholesterol oxidase (31-33), the rate of sterol transfer by
15
16 β -methyl-cyclodextrin (34-37), and the activation of SREBP-2 on the endoplasmic reticulum
17
18 (38).
19
20
21

22 The enzymatic activity of *C. perfringens* α -toxin generates diacylglycerol by releasing the
23
24 phosphocholine head group of PC. Therefore, we reasoned that α -toxin activity may increase the
25
26 amount of free cholesterol in the membrane and assist the interaction of PFO with the cell
27
28 membranes (see Fig. 4 below) (31). This is note-worthy because certain CDCs have been
29
30 reported to act on intracellular membranes which may not ordinarily contain enough cholesterol
31
32 to trigger toxin binding (39-42)
33
34
35
36

37 Our present studies revealed that α -toxin action on membrane bilayers triggers PFO binding
38
39 even in membranes containing low cholesterol levels. These studies suggest a mechanism for the
40
41 concerted action of α -toxin and PFO during *C. perfringens* pathogenesis: the α -toxin activity
42
43 facilitates the exposure of free cholesterol molecules, sensitizing the cell membrane for PFO
44
45 binding and cytolysis.
46
47
48
49
50
51
52
53
54
55
56
57
58
59
60

EXPERIMENTAL PROCEDURES

Preparation of PFO derivatives. The expression and purification of the PFO derivatives was done as described previously (11, 15, 20, 29). The PFO derivative containing the native sequence (amino acids 29-500) plus the polyhistidine tag that came from the pRSETB vector (Invitrogen) is named nPFO. The Cys-less derivative of nPFO (where Cys459 was replaced by Ala) is named rPFO. Since no significant functional or structural differences were found between PFO derivatives bearing or lacking the polyhistidine tag, the nPFO and rPFO derivatives were used in this study directly as purified (11).

Preparation of lipids and liposomes. Non-sterol lipids were obtained from Avanti Polar Lipids (Alabaster, AL) and cholesterol from Steraloids (Newport, RI). Large unilamellar vesicles were prepared with mixtures of 1-palmitoyl-2-oleoyl-*sn*-glycero-3-phosphocholine (POPC), 1-palmitoyl-2-oleoyl-*sn*-glycero-3-phosphoethanolamine (POPE), 1-palmitoyl-2-oleoyl-*sn*-glycerol (DAG), or cholesterol (5-cholesten-3 β -ol), and were generated as described previously (43). Briefly, chloroform solutions of the lipids were combined, shell-dried under nitrogen, rehydrated at ~21-23 °C in buffer A (50mM HEPES, 100mM NaCl, pH 7.5) to 5-30 mM final concentration of total lipids (final volume 0.5 mL), and extruded through 0.1 μ m polycarbonate filters (Avanti Polar Lipids) (44). Reduced L-glutathione (GSH) was labeled with 5-iodoacetamidofluorescein (Fl, Molecular Probes, Invitrogen) by incubating a 1:1 molar ratio mixture in buffer A for 18 h and stored at -20°C until use. β -amylase was labeled with the succinimidyl ester of Oregon Green-488X, 6-isomer (OG, Molecular Probes, Invitrogen) by incubating a 1:1 molar ration mixture in sodium bicarbonate 100 mM pH 8.3. Liposomes encapsulating terbium-dipicolinic acid [Tb(DPA)₃³⁻], GSH-Fl, or β -amylase OG, were prepared as described previously (43).

1
2
3 *Assay for PFO binding.* For the spectroscopic analysis of PFO-membrane interactions,
4 288 μ l aliquots of 200 nM purified PFO in buffer A were distributed into quartz microcells.
5
6 After measuring the initial net (after blank subtraction) fluorescence intensity (F_{sol}) of each
7
8 sample, each cuvette received 12 μ l of 5 mM liposomes (total lipid) to a final concentration of
9
10 200 μ M. The PFO-liposome samples were mixed and incubated at 37°C for 30 min. After
11
12 equilibration to 25°C, the net (after blank subtraction and dilution correction) emission intensity
13
14 (F_{memb}) of each sample was measured. The change in the Trp emission intensity produced by the
15
16 binding of PFO to cholesterol-containing membranes was expressed as $F_{\text{memb}}/F_{\text{sol}}$ (11, 16, 29,
17
18 43).

19
20 *Assay for pore formation.* Pore formation was determined using liposomes loaded with
21
22 GSH-FI, or β -amylase-OG, and an anti-fluorescein antibody added to the external buffer solution
23
24 as a quencher (43). Liposomes (50 μ M total lipids) were suspended in buffer A containing 5 mM
25
26 CaCl_2 and 10 μ l of a 1:10-diluted (in buffer A) solution of anti-fluorescein antibody (0.5 μ l of
27
28 this rabbit polyclonal IgG fraction quenches ~95% of the emission intensity of 0.8 fmol of GSH-
29
30 FI in buffer A; lot 84B1, Molecular Probes, Invitrogen). After thermal equilibration of the
31
32 liposomes at 37°C, a background signal was recorded for 5 min and *C. perfringens* α -toxin
33
34 (Type XIV, Sigma, MO) was added to a final concentration of 0.5 units/ml (1.4 mg/ml, final
35
36 volume 1.6 ml). The signal was continuously recorded and after 15 min of incubation, PFO and
37
38 ethylenedinitrilotetraacetic acid (EDTA) in buffer A were added to a final concentration of 300
39
40 nM and 10 mM, respectively. The PFO dependent release of the encapsulated GSH-FI was
41
42 recorded for an additional 10 min. An identical sample was analyzed but an equivalent volume
43
44 of buffer A was added instead of α -toxin (control). Emission intensities were integrated for 5 sec
45
46 at intervals of 30 sec and recorded. The net emission intensity (F) of the sample at each time
47
48
49
50
51
52
53
54
55
56
57
58
59
60

1
2
3 point was determined after dilution correction. The GSH-FI quenched by the antibody was
4
5 plotted as (F/F_0) , where F is the intensity at any time t , and F_0 is the initial intensity of the
6
7 liposomes. The maximal quenching (F/F_0) for GSH-FI under these experimental conditions is
8
9 typically 0.12 (43). Blank measurements were made using an otherwise identical sample that
10
11 lacked α -toxin and PFO.
12
13

14
15 *Steady-state fluorescence spectroscopy.* Intensity measurements were performed using a
16
17 SLM-8100 spectrofluorimeter as described earlier (20) or a Fluorolog 3-21 spectrofluorimeter
18
19 equipped with a 450 W xenon arc lamp, a double excitation monochromator, a single emission
20
21 monochromator, and a cooled PMT. Unless otherwise indicated, samples were equilibrated to
22
23 25°C before fluorescence determinations. The excitation wavelength and band-pass, and the
24
25 emission wavelength and band-pass, respectively, were: 295, 2, 348, and 4 nm for Trp; 495, 2,
26
27 520, and 2 nm for fluorescein; 492, 2, 518, and 4 for OG. End-point measurements were done in
28
29 4 × 4 mm quartz microcells (43). When additions were made to microcells, the contents were
30
31 mixed thoroughly with a 2 × 2 mm magnetic stirring bar as described previously (45). Kinetics
32
33 measurements were done using 1 × 1 cm quartz cells, and the samples were continuously stirred
34
35 using a magnetic stirring bar (1.5 × 8 mm) (43).
36
37
38
39
40
41

42 For emission spectra determination, aliquots of 2 mL of each PFO derivative were dialyzed
43
44 simultaneously against 4 L of buffer A supplemented with 1 mM (2*S*,3*S*)-1,4-bis-sulfanylbutane-
45
46 2,3-diol (DTT) and 0.5 mM EDTA at 4°C for 10 hr, and clarified by centrifugation at 21000 × g
47
48 for 10 min at 4°C. After dialysis samples were diluted in quartz microcells with dialysis buffer to
49
50 a final concentration of 0.5 μ M (final volume 300 μ L). Spectra for each of these samples were
51
52 recorded at 25°C with the excitation wavelength fixed at 270 nm and a bandpass of 2 nm. The
53
54 emitted light was collected through a vertically oriented Glan-Thompson polarizer (to account
55
56
57
58
59
60

1
2
3 for polarization effects in the emission monochromator) (46) and wavelengths scanned from 280
4 nm to 450 nm using a bandpass of 4 nm. The signal was integrated for 1 sec at intervals of 1 nm.
5
6 Three independent spectra were recorded for the sample containing the toxin and for the control
7
8 sample (dialysis buffer). The emission spectrum of the control sample was subtracted from the
9
10 spectrum of the equivalent sample containing the toxin, and the blank corrected spectrum
11
12 smoothed using a Savitzky-Golay smoothing filter (of degree 2) using a window of 11 points
13
14 (OriginLab software). Fluorescence emission spectra for Trp residues were recorded similarly,
15
16 except that the excitation wavelength was set at 297 nm and the emission wavelength scanned
17
18 from 305 to 450 nm. Total intensity for each sample was calculated as the sum of the intensities
19
20 obtained at each wavelength of the scanned spectrum.
21
22
23
24
25
26

27
28 *Urea unfolding-refolding equilibrium studies.* Unfolding was done by mixing the
29
30 concentrated protein solutions (9-23 μL) into the urea solution (final volume 300 μL , protein
31
32 concentration 0.5 μM). Urea concentration was determined by measuring the refractive index of
33
34 the urea stock solution as described by Pace & Scholtz (47). Both solutions contained buffer A
35
36 supplemented with 1 mM DTT and 0.5 mM EDTA. The proteins were incubated for 12 h at
37
38 23°C-25°C to reach equilibrium. nPFO refolding was done similarly using a stock solution of the
39
40 protein in 6M urea. Trp fluorescence emission spectra were measured at 25 °C in the wavelength
41
42 range 310-450 nm with an excitation wavelength of 297 nm and excitation and emission band-
43
44 pass widths of 4 nm and 8 nm, respectively. Total intrinsic fluorescence emission spectra were
45
46 measured at 25°C in the wavelength range 287-450 nm with an excitation wavelength of 274 nm
47
48 and excitation and emission band-pass widths of 2 nm and 8 nm, respectively. The signal was
49
50 integrated for 1 sec at intervals of 1 nm. Two independent spectra were averaged to reduce
51
52 background noise. The magic angle configuration was used (Glan-Thompson prism polarizers in
53
54
55
56
57
58
59
60

1
2
3 both the excitation, 54.7^o, and emission, 0^o, beams) to assure that the intensity was proportional
4 to the total light intensity of the sample and to correct for spectral distortions caused by the
5 monochromators (46). All spectra were corrected by subtraction of a spectrum of an equivalent
6 buffer solution at the given urea concentration. The observed average energy of emission (or
7 spectral center of mass $\langle\nu_p\rangle$) was calculated according to: $\langle\nu_p\rangle = \sum\nu_i F_i / \sum F$ where F_i stands for
8 the fluorescence emitted at wavenumber ν_i (48). The corresponding wavelength values in nm
9 ($1/\langle\nu_p\rangle$) were used to estimate the conformational stability of the proteins [$\Delta G_{U-F}^{\text{water}}$], assuming
10 a two-state unfolding model for the PFO monomers (49, 50).
11
12
13
14
15
16
17
18
19
20
21
22
23
24
25
26
27
28
29
30
31
32
33
34
35
36
37
38
39
40
41
42
43
44
45
46
47
48
49
50
51
52
53
54
55
56
57
58
59
60

RESULTS

Assessing PFO wild-type binding to membranes using intrinsic fluorescence. When PFO is secreted from *C. perfringens*, the first 28 amino acids required for protein secretion are cleaved (51). Recombinant PFO proteins typically carry a modified N-terminus that contains additional amino acids including a polyhistidine tag and antibody epitope, which extends the native mature sequence by ~30 amino acids. To analyze how the spectroscopic properties of PFO are affected by amino acid modifications we characterized four commonly used PFO derivatives (Table 1, see supporting information): i) the Cys-less original variant of PFO (named pRT20) (20, 52) which contains 36 additional amino acids at the N-terminus, two of which are aromatic and contribute to the spectroscopic signals of the protein (one Trp and one Tyr) (see 11, *for sequence details*); ii) the PFO construct without the non-native Trp residue in the N-terminus (named rPFO or pAH21) (11, 15); iii) the His-tag minus derivative generated by enterokinase cleavage of the first thirty-one amino acids of rPFO, generating a protein that contains aromatic residues identical to the wild-type protein, and only six extra amino acids on its N-terminus (pAH21His) (11) and iv) the native-like PFO derivative originated by reintroduction of the Cys459 residue into the rPFO construct (named nPFO or pAH11) (11, 15).

The emission spectrum for the Cys-less rPFO revealed a small red shift of the emission maximum and an increase in the total fluorescence intensity when compared with nPFO (Table 1). Examination of the three dimensional structure of the PFO monomer (53) showed that the thiol group of Cys459 lies close to the aromatic ring of Trp467. This suggests that the red shift in the emission spectrum and higher fluorescence emission intensity observed for rPFO result mainly from the absence of Cys459 and its thiol group which quenches Trp467. The pRT20 derivative showed an additional red shift in the maximum of the emission spectrum, suggesting

1
2
3 that the extra Trp in the N-terminus of this derivative is located in a polar environment,
4
5 presumably exposed to an aqueous environment as expected for a non-structured segment (53).
6
7

8 We have shown previously that the Trp fluorescence change that follows PFO/membrane
9
10 incubations can be used to quantify toxin binding (11). Since the water-soluble forms of PFO
11
12 employed in our studies differ slightly in their intrinsic fluorescence properties, it is expected
13
14 that the relative emission intensity change observed upon membrane binding, ($F_{\text{memb}}/F_{\text{sol}}$), will
15
16 differ for different PFO derivatives. Therefore, fluorescence intensities were normalized to
17
18 directly compare the binding isotherms for different PFO derivatives (see below).
19
20
21

22 *PFO binding and pore-formation have similar cholesterol dependence.* Studies using
23
24 Intermedilysin, a CDC that requires cholesterol for pore-formation but not for binding, revealed
25
26 that cholesterol plays multiple roles in the CDC mechanism (14). In addition to modulating the
27
28 binding of PFO, cholesterol also seems to be required for the insertion of the amphipathic
29
30 β -hairpins. Does PFO pore-formation have a different cholesterol threshold than the binding to
31
32 membranes? Liposomes formed with different mixtures of POPC and cholesterol were used to
33
34 follow nPFO binding and pore-formation as a function of cholesterol content. Binding was
35
36 followed using the intrinsic Trp fluorescence increment that results from the interaction of PFO
37
38 domain 4 (D4) with the membrane (Fig 1B, filled symbols) (11). For nPFO, membrane binding
39
40 increases sharply above 35 mol% cholesterol with apparent saturation near 45 mol%. PFO pore-
41
42 formation was detected by the decrease in the fluorescence signal (fraction of GSH-Fl quenched)
43
44 caused by the specific binding of the antibody to the fluorescein dye (43). In good agreement
45
46 with the binding data, pore formation was minimal at cholesterol levels below 35 mol%. The
47
48 mid transition to maximal pore-formation occurs at 42 mol% cholesterol, just 2 mol% above the
49
50 mid transition for the binding process. This small effect could be explained by the non-
51
52
53
54
55
56
57
58
59
60

1
2
3 homogeneous distribution of PFO molecules on liposomes containing slightly different amounts
4 of cholesterol. While some vesicles are punctured by more than one pore, others may not bind
5 enough monomers to trigger the insertion of the β -hairpins (21). As observed for the binding
6 measurements, maximal pore-formation was reached as cholesterol approaches 50 mol%. We
7 conclude from these data that if there is enough cholesterol to trigger PFO binding, under
8 conditions that do not preclude pore-formation (like for example low temperature or when using
9 non-lytic PFO variants, 16, 18), pore-formation will occur. Thus, the PFO cytolytic mechanism
10 is modulated by cholesterol at the initial binding step.
11
12
13
14
15
16
17
18
19
20
21

22 *Enhancing free cholesterol molecules promotes PFO binding: effect of POPE.* The
23 appearance of free cholesterol in the membrane is affected by both, the total amount of
24 cholesterol present in the membrane and the overall phospholipid composition of the lipid
25 bilayer (54). Hence, PFO binding can be modulated by changes in the phospholipid composition,
26 like the length of the phospholipid acyl chains and the degree of acyl chain saturation (11, 30,
27 55).
28
29
30
31
32
33
34
35

36 Appearance of free cholesterol molecules in the membrane is also affected by the head
37 group of the phospholipids (56). We therefore quantified how much the change of a choline
38 group, for a smaller ethanolamine group, affected PFO binding at a fixed cholesterol
39 concentration. We prepared membranes containing increasing amounts of POPE (by replacing
40 an equal amount of POPC) at a cholesterol concentration fixed at 35 mol% of the total lipids,
41 and determined the binding of nPFO. When only POPC is present in membranes containing 35
42 mol% cholesterol nPFO does not bind (Fig. 1). However, nPFO started to bind when 30 % of
43 POPC was replaced by POPE (Fig. 1B, POPE 19.5 mol% of the total lipids). Maximal binding
44 was obtained with an equimolar mixture of POPE/POPC. Based on these observations, one
45
46
47
48
49
50
51
52
53
54
55
56
57
58
59
60

1
2
3 would predict that the smaller the head group of the phospholipid, the less cholesterol will be
4 required in the membrane to trigger PFO binding. Does the addition of POPE have any effect on
5 pore formation? As observed for just POPC, binding of PFO to POPC/POPE membranes dictates
6 how much pore formation occurs, as determined by the quenching of the encapsulated marker
7 (Fig. 1B, bars). No pore formation was detected on membranes containing 5 % POPE in the non-
8 sterol lipid fraction, but pore-formation paralleled PFO binding to membranes above 30 %
9 POPE.
10
11
12
13
14
15
16
17
18
19

20 *Enhanced free cholesterol exposure promotes PFO binding: effect of DAG.* Elimination
21 of the phosphocholine group in POPC, which leaves the glycerol backbone plus both acyl-
22 chains, should have a maximal affect on the exposure of free cholesterol molecules and
23 consequent PFO binding. Using a similar approach to that outlined in the previous section we
24 analyzed the binding of nPFO to liposomes prepared with different amounts of POPC and DAG
25 (Fig. 1C, open circles).
26
27
28
29
30
31
32
33

34 Surprisingly, the threshold for PFO binding was abruptly achieved as the membrane
35 population of DAG composes only 5 mol% of the total lipids, with saturation levels reached at
36 approximately 13 mol% DAG. The replacement of small amounts of POPC by DAG was enough
37 to enhance the exposure of free cholesterol molecules and trigger PFO binding. As observed for
38 the analysis of POPE, pore formation paralleled the binding of nPFO at different DAG
39 concentrations (Fig. 1C, bars).
40
41
42
43
44
45
46
47

48 The above results confirmed that at a fixed cholesterol concentration, the smaller the
49 phospholipid head of the added glycerolipid, the lower the threshold for PFO binding. Binding
50 of PFO to membrane bilayers can therefore, be modulated by the overall lipid composition rather
51 than solely by the total cholesterol content.
52
53
54
55
56
57
58
59
60

1
2
3
4
5
6
7
8
9
10
11
12
13
14
15
16
17
18
19
20
21
22
23
24
25
26
27
28
29
30
31
32
33
34
35
36
37
38
39
40
41
42
43
44
45
46
47
48
49
50
51
52
53
54
55
56
57
58
59
60

Cholesterol dependence of the Cys-less PFO mutant rPFO. Most of the structural and mechanistic studies of PFO have been done with a Cys-less derivative rPFO, where the unique and conserved Cys459 was replaced by Ala (11, 15-17, 19-22, 29, 43). Both nPFO and rPFO have similar hemolytic activity and efficiently bind to liposomes containing high cholesterol (more than 50 mol% cholesterol) (20). Based on these observations, it has been commonly assumed that the binding properties of the Cys less derivatives for some CDCs were the same. However, we noticed that the cholesterol-dependent binding of these two PFO derivatives has different sterol concentration threshold (Fig 2A and Fig. 3). The C459A mutant rPFO required ~5 mol% more cholesterol to trigger binding to POPC:cholesterol liposomes as compared with nPFO.

We therefore asked if the C459A mutation affected the conformational stability of the toxin. It was found that, despite causing a small but significant change in the cholesterol-dependent binding properties of PFO, the C459A mutation did not alter the stability of the toxin, as determined by the equilibrium urea denaturation of the monomeric protein (Fig. 2C) (49, 50, 57). nPFO unfolding by urea was reversible, with a $\Delta G_{U-F}^{\text{water}} = 11 \pm 3 \text{ kcal mol}^{-1}$ (Fig. 2B). The data were fitted assuming a two state model, and similar results were obtained whether we measured the changes in the average energy of emission (Fig. 2B and 2C) or the total fluorescence intensity under the spectrum (data not shown) (49). The whole PFO molecule unfolded cooperatively as indicated by the similar concentration of urea required for 50% unfolding when only Trp were excited at 297 nm (Fig. 2B), or when all aromatic amino acids were excited at 274 nm (data not shown). While Trp fluorescence reports mostly the unfolding of D4 (six of the seven Trp residues are located in this domain), excitation at 274 nm reports the

1
2
3 unfolding of the overall molecule (23 Tyr residues are distributed all over the molecule, Table
4
5 S1 supporting information).
6

7
8 The change of the conserved Cys459 to Ala neither affected the stability of the PFO
9
10 molecule nor the activity of PFO at high cholesterol concentration. However, it is clear that this
11
12 residue contributes to the ability of PFO to interact with cholesterol when the membrane
13
14 contains lower cholesterol levels.
15
16

17
18 *C. perfringens* α -toxin facilitates PFO membrane interaction. α -Toxin alters the
19
20 properties of the target cell membrane by removing the phosphocholine moieties from PC and
21
22 SM. As a consequence of the head-group removal, more free cholesterol molecules appear in the
23
24 membrane. Does the α -toxin modification of the membrane facilitate PFO binding and pore-
25
26 formation as a result of the increase in the number of free cholesterol?
27
28

29
30 PFO binding changes abruptly from no binding to complete binding in a very narrow
31
32 range of cholesterol concentrations (only a 10 mol % cholesterol increment). To evaluate how
33
34 α -toxin activity affects the number of free cholesterol molecules present in the membrane, we
35
36 measured the affect of α -toxin on PFO activity using membranes containing cholesterol
37
38 concentrations just below the binding threshold. We measured the kinetics of pore formation for
39
40 both nPFO and rPFO derivatives, on membranes treated, or non-treated, with α -toxin. The extent
41
42 of PFO pore-formation on untreated liposomes (Fig. 3, filled symbols) correlated well with the
43
44 extent of binding observed for these PFO derivatives (Fig. 2A).
45
46
47

48
49 A baseline signal was measured during 5 min before the addition of α -toxin (Fig. 3 open
50
51 circles), or the addition of an equivalent amount of buffer A (control, Fig. 3 filled circles). Some
52
53 quenching of GSH-FI was observed during α -toxin incubations. The origin for the GSH-FI
54
55 leakage is not known, but it may be caused by the fusion of some vesicles (58, 59), or by
56
57
58
59
60

1
2
3 nonspecific GSH-FI leakage through transient disruptions caused by α -toxin. The amount and
4 rate of leakage of GSH-FI was independent of the cholesterol concentration (Fig. 3, open circles
5
6 between 5 and 20 min), but dependent on the concentration of α -toxin (Fig. 2S, supporting
7
8 information). Similar leakage was observed when a larger reporter, β -amylase-OG (ca. 100Å vs.
9
10 ca. 10Å for GSH-FI), was encapsulated in the liposomes, indicating that both small and large
11
12 molecules were released and quenched by the anti-FI/OG-antibody (ca. ~120 Å) (43) as a
13
14 consequence of the α -toxin activity (data not shown).
15
16
17
18
19

20
21 After 15 min of incubation with α -toxin, PFO and EDTA were simultaneously added
22
23 (the latter to chelate Ca^{2+} ions and thus inhibit α -toxin) (60) and pore formation followed for 10
24
25 additional minutes. An increase in the extent of pore formation was observed for both PFO
26
27 derivatives when membranes containing more than 30 mol% cholesterol were previously
28
29 exposed to α -toxin (compare open vs. filled circles in Fig. 3). When only EDTA was added
30
31 (control with no PFO), no significant change was observed in GSH-FI quenching (Fig. 3E, solid
32
33 line). The closer the cholesterol concentration approached the threshold required to trigger PFO
34
35 binding, the more prominent was the effect of α -toxin. In particular for rPFO, note that the
36
37 extent of pore formation increased more than 3-fold when liposomes containing 40 mol%
38
39 cholesterol were pre-incubated with α -toxin (Fig. 3F).
40
41
42
43
44

45
46 In agreement with the data obtained with liposomes prepared with POPE or DAG (Fig
47
48 1B and 1C), hydrolysis of the phosphocholine group from POPC by α -toxin increased the
49
50 amount of free cholesterol molecules in the membrane and as a consequence facilitated PFO
51
52 binding and pore formation.
53
54
55
56
57
58
59
60

DISCUSSION

Our examination of the cholesterol dependence of PFO binding and pore-formation has provided four primary insights into the mechanism of PFO interaction with cholesterol in membrane bilayers. First, cholesterol-dependent PFO pore formation is regulated at the initial binding step of the cytolytic mechanism. Second, the amount of cholesterol required to trigger PFO binding to membranes is reduced when phospholipids with smaller head groups are present (e.g., DAG or POPE, compared to POPC). Third, the conserved Cys459 is important for cholesterol recognition in membranes containing low cholesterol levels. Fourth, α -toxin activity (i.e., hydrolysis and release of phospholipid head-groups) facilitates PFO cytolytic activity in membranes containing low cholesterol content. In addition, we have determined that the chemical denaturation and refolding of the PFO monomer by urea is a reversible process, with a $\Delta G_{U-F}^{\text{water}} = 11 \pm 3 \text{ kcal mol}^{-1}$.

Cholesterol is essential for PFO cytolysis; however the exact mechanism for this specific protein-lipid interaction remains elusive (9, 61, 62). It has become clear that the organization of the cholesterol molecules in the membrane bilayer (11, 30, 56, 63) and the conformation of the loops located in the tip of PFO D4 play an important role on this interaction (12, 13, 23).

PFO binds directly to pure cholesterol aggregates in aqueous solutions, but not when cholesterol is complexed with phospholipids or shielded from the membrane surface (Fig. 4A) (16, 29, 56). The minimal amount of cholesterol required to trigger PFO membrane binding is determined by the interactions between the sterol molecules and the phospholipids (11, 30). Less cholesterol is required in the membrane when the liposomes contain unsaturated phospholipids rather than phospholipids with saturated acyl chains. The kinks introduced by the double bonds reduce the area of interaction between the acyl chains and the sterol. Consequently, free

1
2
3 cholesterol molecules become more readily available to interact with PFO. In accordance with
4 these observations, molecules that intercalate with the phospholipids but do not interact with
5 PFO move the cholesterol binding threshold to lower cholesterol concentrations (11, 64). A
6 typical binding isotherm for nPFO to POPC membranes prepared with increasing amounts of
7 cholesterol is shown in Fig. 1A. Under these conditions, PFO requires at least 35 mol%
8 cholesterol in the membrane before any binding is detectable (16). Once the binding threshold is
9 achieved there is a relatively narrow range required to reach saturation. This cooperative binding
10 behavior is characteristic of several CDCs like tetanolysin (65), SLO (66), and LLO (67).
11
12
13
14
15
16
17
18
19
20
21

22 Binding of individual PFO monomers to the membrane surface is followed by
23 oligomerization and the formation of the pre-pore complex (18, 43). The final step of the
24 cytolytic mechanism is the cooperative insertion of two amphipathic β -hairpins per monomer to
25 form a transmembrane β -barrel (19, 68). A comparative analysis between PFO and
26 intermedilysin (a CDC secreted by *Streptococcus intermedius*), showed that the initial and final
27 steps of the cytolytic mechanism are sensitive to the total cholesterol content in the bilayer (14).
28 To investigate how cholesterol affects each of these steps, both binding and pore-formation were
29 measured using membranes with identical lipid composition. As shown in Fig. 1, no significant
30 differences were observed for the binding and the pore formation activity of PFO. The small
31 difference observed between binding and pore formation can be explained by a non-
32 heterogeneous distribution of PFO among the vesicles, or alternatively, by the presence of a
33 small number of non-inserted incomplete oligomers. Hence, we concluded that the initial step of
34 the cytolytic mechanism (i.e., cholesterol-dependent binding) determines the ability of PFO to
35 form pores in membranes. What membrane factors affect the PFO/membrane interaction?
36
37
38
39
40
41
42
43
44
45
46
47
48
49
50
51
52
53
54
55
56
57
58
59
60

1
2
3 Both, acyl chain length and saturation have been argued to vary the amount of free
4 cholesterol molecules in the membrane (37), thus affecting PFO binding. As suggested for SLO
5 (56), we reasoned that structural changes in the phospholipid head-groups could likewise affect
6 cholesterol distribution and therefore toxin binding (69). We therefore quantified the effect of
7 the head-groups on PFO binding using membranes containing low cholesterol levels.
8 Maintaining the cholesterol concentration constant at 35 mol% of the total lipids, we gradually
9 replaced some of the POPC content by POPE, and PFO binding was observed only when the
10 POPE/POPC ratio was higher than 1/3; with apparent saturation achieved at equimolar
11 concentrations (Fig. 1B). The acyl chains of POPE are identical to those of POPC, thus any
12 effect on the PFO-cholesterol interaction would be a result of the different head-group. A
13 parsimonious explanation for these data is that the comparatively diminutive ethanolamine head-
14 group provides less shielding bulk for the cholesterol molecule (28, 56). Alternatively, this
15 observation can also be explained if POPE does not associate as effectively with cholesterol as
16 POPC does, and therefore the amount of free cholesterol molecules increase, as reflected by the
17 boost in the binding of the PFO molecules to the bilayer (35). At this point we cannot rule out
18 the possibility that micro-heterogeneities may exist in the lipid mixtures at high cholesterol
19 concentrations that may also explain the observed binding behavior, like the presence of
20 undetectable nano-domains or cholesterol crystals (70, 71).
21
22
23
24
25
26
27
28
29
30
31
32
33
34
35
36
37
38
39
40
41
42
43
44

45
46 Are there any processes that may affect the phospholipid head-group distribution during
47 *C. perfringens* pathogenesis? *C. perfringens* α -toxin is a phospholipase C which cleaves the
48 head-group from POPC leaving a DAG moiety in the membrane, certainly the sparsest form of a
49 diacyl lipid (Fig. 4B). Since the removal of the phospholipid head-group will increase the
50 amount of free cholesterol in the membrane, we quantified the effect of replacing POPC for
51
52
53
54
55
56
57
58
59
60

1
2
3 DAG on PFO binding. POPC liposomes with 35 mol% cholesterol were used as for the analysis
4 of POPE. POPC was substituted by DAG in a step-wise fashion. Interestingly, the binding
5 threshold was reached when DAG constituted just 5 mol% of the total lipids. Binding saturation
6 was reached when DAG concentration was ~13 mol% of the total lipids (i.e., DAG/POPC ratio
7 of 1/5). When the above experiments were repeated but with liposomes containing 25 mol%
8 cholesterol, a concentration far below the binding threshold level, PFO binding was nevertheless
9 educed when DAG/POPC ratio was higher than 1/3 (data not shown). This effect clearly echoes
10 observations with POPE with the attendant rationale – free cholesterol molecules become
11 available for PFO binding. Is the availability of free cholesterol the only requisite to trigger PFO
12 binding? Does the conserved Cys play any role in cholesterol recognition?
13
14
15
16
17
18
19
20
21
22
23
24
25
26

27 The tip of PFO D4 contains regions of conservation that suggest a vital role for this
28 domain. A conserved undecapeptide was found to be very important for PFO activity and
29 binding (72), and it has long been suggested that this segment may constitute the binding site for
30 a cholesterol molecule (73). However, it has been recently implied that the PFO undecapeptide is
31 uncoupled from toxin membrane binding (12). Instead, the Thr 490 and Leu 491 residues located
32 in D4/loop 1 of PFO appear to mediate PFO binding to membranes containing high cholesterol
33 (23). Interestingly, we report here that the cholesterol binding properties of the undecapeptide
34 C459A mutant differs from that observed for the native form of PFO. While the mutation neither
35 affected the conformational stability of PFO (Fig. 2C) nor the PFO binding at high cholesterol
36 concentration (20, 74-77), elimination of the thiol group at residue 459 elevated the binding
37 threshold for cholesterol by 5 mol% (Fig. 2A). This observation suggests that binding of PFO to
38 cholesterol-containing membranes may not be completely independent of the conserved
39 undecapeptide. This segment may not be only important for the insertion of the β -hairpins (12),
40
41
42
43
44
45
46
47
48
49
50
51
52
53
54
55
56
57
58
59
60

1
2
3 but also to modulate how much cholesterol is require on the membrane to trigger binding. The
4 role of the Cys may be critical when the CDC act on membranes containing low cholesterol
5 levels, as it has been suggested for LLO (78).
6
7
8
9

10 The concentration of cholesterol in human red blood cells is approximately 45 mol% of
11 the total lipid (79), and these cells are frequently used to evaluate the activity of different PFO
12 derivatives (20, 76, 80). Is worth to notice that the cholesterol content of red blood cells is 7-10
13 mol% higher than the cholesterol content of macrophages (81), cells that are a physiological
14 target for PFO. While the C459A mutation may not significantly affect the binding to red blood
15 cells, it may affect the binding to other cells (or to intracellular membranes) that contain lower
16 cholesterol levels.
17
18
19
20
21
22
23
24
25
26

27 PFO is secreted by *C. perfringens* to the extracellular medium as an unfolded
28 polypeptide (51, 82). Outside the cell, the toxin spontaneously folds into a rod-shape molecule
29 with three discontinues domains (domains 1 to 3) and a compact C-terminal β -sandwich (or D4,
30 residues 391-500, see Fig. 4A) (53). Our urea denaturation studies showed that the protein
31 refolds *in vitro* after dilution of the denaturing agent (Fig. 2B), accordingly with the spontaneous
32 tendency of the polypeptide to adopt its three dimensional structure. The free energy of
33 unfolding in water was $11 \pm 3 \text{ kcal mol}^{-1}$, assuming a two-state transition for the unfolding
34 equilibrium of the toxin. No significant differences were found in the conformational stability of
35 the rPFO derivative, where the conserved Cys459 was mutated to Ala, when compare with the
36 native-like nPFO derivative. The similarity among the thermodynamic parameters of the two
37 PFO derivatives suggests that no major conformational changes are introduced by this mutation.
38
39
40
41
42
43
44
45
46
47
48
49
50
51
52

53 Pathogenesis by *C. perfringens* is mediated by two potent exotoxins; α -toxin, and PFO.
54 While active individually, it has been shown that they exert a synergic effect during *C.*
55
56
57
58
59
60

1
2
3 *perfringens* infections (25, 40, 83). Could α -toxin hydrolysis of phospholipids facilitate the
4
5 cholesterol-dependent interaction of PFO with the membrane? To determine whether the α -toxin
6
7 activity will increase the amount of free cholesterol in the membrane, and a concomitant increase
8
9 in PFO binding, membranes containing different amounts of cholesterol were treated with
10
11 α -toxin and subsequently exposed to PFO. We found that even at cholesterol levels below the
12
13 usual binding threshold, α -toxin pre-incubation appears to poise membranes for PFO lysis (Fig.
14
15 3).

16
17
18
19
20
21 Our results revealed that the effect of α -toxin was more pronounced at cholesterol
22
23 concentrations just below the binding threshold (Fig. 3D-F). No significant effect was observed
24
25 on membranes containing 25 mol% cholesterol (Fig 3A). The lack of synergism at low
26
27 cholesterol concentrations could be explained by the rapid flip-flop movement of the cholesterol
28
29 molecules across the membrane bilayer. Free cholesterol molecules generated on the outer leaflet
30
31 of the bilayer will rapidly equilibrate and form complexes with the excess of phospholipids still
32
33 present in the inner leaflet of the bilayer (36). This is in contrast to the DAG titration
34
35 experiments (Fig. 1C), where the DAG molecules were equally distributed in both leaflets of the
36
37 bilayer. Thus, observations from the DAG titration experiments appear to have a biological
38
39 parallel with the lipolytic degradation of POPC by α -toxin with subsequent sensitization to PFO
40
41 binding and pore-formation. These results suggest that the basis of α -toxin and PFO synergy lies
42
43 in the augment of free cholesterol molecules present in the membrane (Fig. 4).

44
45
46
47
48
49 In summary, the data presented here reveal that α -toxin activity facilitates PFO cytotoxicity
50
51 on membranes that contain low cholesterol levels. In addition, we showed that the binding
52
53 threshold for cholesterol can be modulated by modifications in the undecapeptide. These
54
55 polypeptides are highly conserved among the CDCs (9) and their interaction with the membrane
56
57
58
59
60

1
2
3 may be modulated by changes in the pH of the medium (30, 67). We speculate that these effects
4
5 are responsible for the activity of CDCs on intracellular membranes, which contain much less
6
7 cholesterol than the plasma membrane (84). Interestingly, both PFO and α -toxin have been
8
9 reported to be important for the *C. perfringens* escape from the phagosome (39, 40), and both
10
11 toxins have optimal activity at a mildly acidic pH (30, 85).
12
13

14
15 It is also important to note that LLO, a CDC secreted by *Listeria monocytogenes*, is
16
17 essential for the phagosomal escape of this pathogen (41, 42). Interestingly, LLO and two
18
19 phospholipases (PI-PLC and PC-PLC) are required to effectively dissolve the double-membrane
20
21 spreading vacuole and evade host-cell defense mechanisms (86-89). The action of these
22
23 phospholipases may increase the amount of free cholesterol in the membrane and trigger LLO
24
25 binding and pore formation in cellular vacuoles, even at a suboptimal pH (67). Hence, the results
26
27 reported here are not limited to *C. perfringens* pathogenesis, and they may be generally
28
29 applicable to the pathogenic mechanisms of other bacteria, as well as other cellular processes
30
31 where the action of phospholipases may be coupled to cholesterol dependent protein-membrane
32
33 interactions (90).
34
35
36
37
38
39
40
41

42 **SUPPORTING INFORMATION AVAILABLE**

43
44
45 Effect of the time of pre-incubation with α -toxin on the PFO pore formation activity. Effect of
46
47 the concentration of α -toxin on the sensitization of liposomes to PFO pore formation. List of
48
49 aromatic residues present in each PFO derivative, molar absorptivities values for each PFO
50
51 derivative, and the absorption lambda maximum for each PFO derivative. This material is
52
53 available free of charge via the Internet at <http://pubs.acs.org>.
54
55
56
57
58
59
60

REFERENCES

- (1) Hickey, M. J., Kwan, R. Y. Q., Awad, M. M., Kennedy, C. L., Young, L. F., Hall, P., Cordner, L. M., Lyras, D., Emmins, J. J., and Rood, J. I. (2008) Molecular and cellular basis of microvascular perfusion deficits induced by *Clostridium perfringens* and *Clostridium septicum*. *PLoS Pathogens* 4, e1000045.
- (2) Bryant, A. E., and Stevens, D. L. (2006) Clostridial toxins in the pathogenesis of gas gangrene., in *The comprehensive sourcebook of bacterial protein toxins* (Alouf, J. E., and Popoff, M. R., Eds.) pp 919-929, Academic Press.
- (3) Awad, M. M., Bryant, A. E., Stevens, D. L., and Rood, J. I. (1995) Virulence studies on chromosomal alpha-toxin and theta-toxin mutants constructed by allelic exchange provide genetic evidence for the essential role of alpha-toxin in *Clostridium perfringens*-mediated gas gangrene. *Mol. Microbiol.* 15, 191-202.
- (4) Bunting, M., Lorant, D. E., Bryant, A. E., Zimmerman, G. A., McIntyre, T. M., Stevens, D. L., and Prescott, S. M. (1997) Alpha toxin from *Clostridium perfringens* induces proinflammatory changes in endothelial cells. *J.Clin. Invest.* 100, 565-574.
- (5) Ochi, S., Miyawaki, T., Matsuda, H., Oda, M., Nagahama, M., and Sakurai, J. (2002) *Clostridium perfringens* alpha-toxin induces rabbit neutrophil adhesion. *Microbiology* 148, 237-245.
- (6) Naylor, C. E., Eaton, J. T., Howells, A., Justin, N., Moss, D. S., Titball, R. W., and Basak, A. K. (1998) Structure of the key toxin in gas gangrene. *Nat. Struct. Biol.* 5, 738-746.
- (7) Tweten, R. K. (2005) Cholesterol-dependent cytolysins, a family of versatile pore-forming toxins. *Infect. Immun.* 73, 6199-6209.

- 1
2
3
4
5
6
7
8
9
10
11
12
13
14
15
16
17
18
19
20
21
22
23
24
25
26
27
28
29
30
31
32
33
34
35
36
37
38
39
40
41
42
43
44
45
46
47
48
49
50
51
52
53
54
55
56
57
58
59
60
- (8) Gilbert, R. J. (2010) Cholesterol-dependent cytolysins. *Adv. Exp. Med. Biol.* 677, 56-66.
- (9) Heuck, A. P., Moe, P. C., and Johnson, B. B. (2010) The cholesterol-dependent cytolysins family of Gram-positive bacterial toxins, in *Cholesterol binding proteins and cholesterol transport* (Harris, J. R., Ed.) pp 551-577, Springer.
- (10) Heuck, A. P., Tweten, R. K., and Johnson, A. E. (2001) Beta-barrel pore-forming toxins: Intriguing dimorphic proteins. *Biochemistry* 40, 9065-9073.
- (11) Flanagan, J. J., Tweten, R. K., Johnson, A. E., and Heuck, A. P. (2009) Cholesterol exposure at the membrane surface is necessary and sufficient to trigger perfringolysin O binding. *Biochemistry* 48, 3977-3987.
- (12) Soltani, C. E., Hotze, E. M., Johnson, A. E., and Tweten, R. K. (2007) Structural elements of the cholesterol-dependent cytolysins that are responsible for their cholesterol-sensitive membrane interactions. *Proc. Natl. Acad. Sci. U. S. A.* 104, 20226-20231.
- (13) Soltani, C. E., Hotze, E. M., Johnson, A. E., and Tweten, R. K. (2007) Specific protein-membrane contacts are required for prepore and pore assembly by a cholesterol-dependent cytolysin. *J. Biol. Chem.* 282, 15709-15716.
- (14) Giddings, K. S., Johnson, A. E., and Tweten, R. K. (2003) Redefining cholesterol's role in the mechanism of the cholesterol-dependent cytolysins. *Proc. Natl. Acad. Sci. U. S. A.* 100, 11315-11320.
- (15) Ramachandran, R., Heuck, A. P., Tweten, R. K., and Johnson, A. E. (2002) Structural insights into the membrane-anchoring mechanism of a cholesterol-dependent cytolysin. *Nat. Struct. Mol. Biol.* 9, 823-827.

- 1
2
3
4
5
6
7
8
9
10
11
12
13
14
15
16
17
18
19
20
21
22
23
24
25
26
27
28
29
30
31
32
33
34
35
36
37
38
39
40
41
42
43
44
45
46
47
48
49
50
51
52
53
54
55
56
57
58
59
60
- (16) Heuck, A. P., Hotze, E. M., Tweten, R. K., and Johnson, A. E. (2000) Mechanism of membrane insertion of a multimeric β -barrel protein: Perfringolysin O creates a pore using ordered and coupled conformational changes. *Mol. Cell* 6, 1233-1242.
- (17) Hotze, E. M., Wilson-Kubalek, E. M., Rossjohn, J., Parker, M. W., Johnson, A. E., and Tweten, R. K. (2001) Arresting pore formation of a cholesterol-dependent cytolysin by disulfide trapping synchronizes the insertion of the transmembrane beta-sheet from a prepore intermediate. *J. Biol. Chem.* 276, 8261-8268.
- (18) Shepard, L. A., Shatursky, O., Johnson, A. E., and Tweten, R. K. (2000) The mechanism of pore assembly for a cholesterol-dependent cytolysin: Formation of a large prepore complex precedes the insertion of the transmembrane beta-hairpins. *Biochemistry* 39, 10284-10293.
- (19) Shatursky, O., Heuck, A. P., Shepard, L. A., Rossjohn, J., Parker, M. W., Johnson, A. E., and Tweten, R. K. (1999) The mechanism of membrane insertion for a cholesterol-dependent cytolysin: A novel paradigm for pore-forming toxins. *Cell* 99, 293-299.
- (20) Shepard, L. A., Heuck, A. P., Hamman, B. D., Rossjohn, J., Parker, M. W., Ryan, K. R., Johnson, A. E., and Tweten, R. K. (1998) Identification of a membrane-spanning domain of the thiol-activated pore-forming toxin *Clostridium perfringens* perfringolysin O: An alpha-helical to beta-sheet transition identified by fluorescence spectroscopy. *Biochemistry* 37, 14563-14574.
- (21) Czajkowsky, D. M., Hotze, E. M., Shao, Z., and Tweten, R. K. (2004) Vertical collapse of a cytolysin prepore moves its transmembrane beta-hairpins to the membrane. *EMBO J.* 23, 3206-3215.

- 1
2
3 (22) Dang, T. X., Hotze, E. M., Rouiller, I., Tweten, R. K., and Wilson-Kubalek, E. M. (2005)
4
5
6
7
8
9
10
11 (23) Farrand, A. J., LaChapelle, S., Hotze, E. M., Johnson, A. E., and Tweten, R. K. (2010)
12
13
14
15
16
17
18 (24) Ramachandran, R., Tweten, R. K., and Johnson, A. E. (2004) Membrane-dependent
19
20
21
22
23
24
25 (25) Awad, M. M., Ellemor, D. M., Boyd, R. L., Emmins, J. J., and Rood, J. I. (2001)
26
27
28
29
30
31
32 (26) Heuck, A. P., and Johnson, A. E. (2005) Membrane recognition and pore formation by
33
34
35
36
37
38
39 (27) Radhakrishnan, A., and McConnell, H. M. (1999) Condensed complexes of cholesterol
40
41
42
43
44 (28) Huang, J., and Feigenson, G. W. (1999) A microscopic interaction model of maximum
45
46
47
48
49 (29) Heuck, A. P., Savva, C. G., Holzenburg, A., and Johnson, A. E. (2007) Conformational
50
51
52
53
54
55
56
57
58
59
60
- Prepore to pore transition of a cholesterol-dependent cytolysin visualized by electron microscopy. *J. Struct. Biol.* *150*, 100-108.
- Only two amino acids are essential for cytolytic toxin recognition of cholesterol at the membrane surface. *Proc. Natl. Acad. Sci. U. S. A.* *107*, 4341-4346.
- Membrane-dependent conformational changes initiate cholesterol-dependent cytolysin oligomerization and intersubunit beta-strand alignment. *Nat. Struct. Mol. Biol.* *11*, 697-705.
- Synergistic effects of alpha-toxin and perfringolysin O in *Clostridium perfringens*-mediated gas gangrene. *Infect. Immun.* *69*, 7904-7910.
- Membrane recognition and pore formation by bacterial pore-forming toxins, in *Protein-lipid interactions. From membrane domains to cellular networks* (Tamm, L. K., Ed.) pp 163-186, Wiley-VCH, Weinheim.
- Condensed complexes of cholesterol and phospholipids. *Biophys. J.* *77*, 1507-1517.
- A microscopic interaction model of maximum solubility of cholesterol in lipid bilayers. *Biophys. J.* *76*, 2142-2157.
- Conformational changes that effect oligomerization and initiate pore formation are triggered throughout perfringolysin O upon binding to cholesterol. *J. Biol. Chem.* *282*, 22629-22637.

- 1
2
3
4 (30) Nelson, L. D., Johnson, A. E., and London, E. (2008) How interaction of perfringolysin
5 O with membranes is controlled by sterol structure, lipid structure, and physiological low
6 pH: Insights into the origin of perfringolysin O-lipid raft interaction *J. Biol. Chem.* *283*,
7
8 4632-4642.
9
10
11
12 (31) Moore, N. F., Patzer, E. J., Barenholz, Y., and Wagner, R. R. (1977) Effect of
13 phospholipase C and cholesterol oxidase on membrane integrity, microviscosity, and
14 infectivity of vesicular stomatitis virus. *Biochemistry* *16*, 4708-4715.
15
16
17 (32) Patzer, E. J., and Wagner, R. R. (1978) Cholesterol oxidase as a probe for studying
18 membrane organisation. *Nature* *274*, 394-395.
19
20
21 (33) Ali, M. R., Cheng, K. H., and Huang, J. (2007) Assess the nature of cholesterol-lipid
22 interactions through the chemical potential of cholesterol in phosphatidylcholine bilayers.
23
24
25
26
27
28
29
30
31
32 (34) Ohvo, H., and Slotte, J. P. (1996) Cyclodextrin-mediated removal of sterols from
33 monolayers: Effects of sterol structure and phospholipids on desorption rate.
34
35
36
37
38
39 (35) Radhakrishnan, A., and McConnell, H. M. (2000) Chemical activity of cholesterol in
40 membranes. *Biochemistry* *39*, 8119-8124.
41
42
43 (36) Leventis, R., and Silvius, J. R. (2001) Use of cyclodextrins to monitor transbilayer
44 movement and differential lipid affinities of cholesterol. *Biophys. J.* *81*, 2257-2267.
45
46
47
48 (37) Lange, Y., and Steck, T. L. (2008) Cholesterol homeostasis and the escape tendency
49 (activity) of plasma membrane cholesterol. *Prog. Lipid Res.* *47*, 319-332.
50
51
52
53
54
55
56
57
58
59
60

- 1
2
3
4
5
6
7
8
9
10
11
12
13
14
15
16
17
18
19
20
21
22
23
24
25
26
27
28
29
30
31
32
33
34
35
36
37
38
39
40
41
42
43
44
45
46
47
48
49
50
51
52
53
54
55
56
57
58
59
60
- (38) Sokolov, A., and Radhakrishnan, A. (2010) Accessibility of cholesterol in endoplasmic reticulum (ER) membranes and activation of srebp-2 switch abruptly at a common cholesterol threshold. *J. Biol. Chem.* Jun 23. [Epub ahead of print]
- (39) O'Brien, D. K., and Melville, S. B. (2000) The anaerobic pathogen clostridium perfringens can escape the phagosome of macrophages under aerobic conditions. *Cell. Microbiol.* 2, 505-519.
- (40) O'Brien, D. K., and Melville, S. B. (2004) Effects of clostridium perfringens alpha-toxin (PLC) and perfringolysin O (PFO) on cytotoxicity to macrophages, on escape from the phagosomes of macrophages, and on persistence of *C. perfringens* in host tissues. *Infect. Immun.* 72, 5204-5215.
- (41) Vazquez-Boland, J. A., Kuhn, M., Berche, P., Chakraborty, T., Dominguez-Bernal, G., Goebel, W., Gonzalez-Zorn, B., Wehland, J., and Kreft, J. (2001) *Listeria* pathogenesis and molecular virulence determinants. *Clin. Microbiol. Rev.* 14, 584-640.
- (42) Schnupf, P., and Portnoy, D. A. (2007) Listeriolysin O: A phagosome-specific lysin. *Microb. Infect.* 9, 1176-1187.
- (43) Heuck, A. P., Tweten, R. K., and Johnson, A. E. (2003) Assembly and topography of the prepore complex in cholesterol-dependent cytolysins. *J. Biol. Chem.* 278, 31218-31225.
- (44) Mayer, L. D., Hope, M. J., and Cullis, P. R. (1986) Vesicles of variable sizes produced by a rapid extrusion procedure. *Biochim. Biophys. Acta* 858, 161-168.
- (45) Ye, J., Esmon, N. L., Esmon, C. T., and Johnson, A. E. (1991) The active site of thrombin is altered upon binding to thrombomodulin: Two distinct structural changes are detected by fluorescence, but only one correlates with protein C activation. *J. Biol. Chem.* 266, 23016-23021.

- 1
2
3 (46) Jameson, D. M., Croney, J. C., Moens, P. D. J., and Gerard Marriott and Ian, P. (2003)
4
5 Fluorescence: Basic concepts, practical aspects, and some anecdotes. *Methods Enzymol.*
6
7 360, 1-43.
8
9
10 (47) Pace, C. N., and Scholtz, J. M. (1989) Measuring conformational stability of a protein, in
11
12 *Protein structure: A practical approach* (Creighton, T. E., Ed.) pp 299-321, Oxford
13
14 University Press.
15
16
17 (48) Bortoleto, R. K., de Oliveira, A. H., Ruller, R., Arni, R. K., and Ward, R. J. (1998)
18
19 Tertiary structural changes of the alpha-hemolysin from *Staphylococcus aureus* on
20
21 association with liposome membranes. *Arch. Biochem. Biophys.* 351, 47-52.
22
23
24 (49) Santoro, M. M., and Bolen, D. W. (1988) Unfolding free energy changes determined by
25
26 the linear extrapolation method. 1. Unfolding of phenylmethanesulfonyl alpha-
27
28 chymotrypsin using different denaturants. *Biochemistry* 27, 8063-8068.
29
30
31 (50) Pace, C. N., and C. H. W. Hirs, S. N. T. (1986) Determination and analysis of urea and
32
33 guanidine hydrochloride denaturation curves. *Methods Enzymol.* 131, 266-280.
34
35
36 (51) Tweten, R. K. (1988) Nucleotide sequence of the gene for perfringolysin O (theta-toxin)
37
38 from *Clostridium perfringens*: Significant homology with the genes for streptolysin O
39
40 and pneumolysin. *Infect. Immun.* 56, 3235-3240.
41
42
43 (52) Tweten, R. K. (1988) Cloning and expression in *Escherichia coli* of the perfringolysin O
44
45 (theta-toxin) gene from *Clostridium perfringens* and characterization of the gene product.
46
47 *Infect. Immun.* 56, 3228-3234.
48
49
50 (53) Rossjohn, J., Feil, S. C., McKinstry, W. J., Tweten, R. K., and Parker, M. W. (1997)
51
52 Structure of a cholesterol-binding, thiol-activated cytolysin and a model of its membrane
53
54 form. *Cell* 89, 685-692.
55
56
57
58
59
60

- 1
2
3
4
5
6
7
8
9
10
11
12
13
14
15
16
17
18
19
20
21
22
23
24
25
26
27
28
29
30
31
32
33
34
35
36
37
38
39
40
41
42
43
44
45
46
47
48
49
50
51
52
53
54
55
56
57
58
59
60
- (54) Lange, Y., Ye, J., Duban, M.-E., and Steck, T. L. (2009) Activation of membrane cholesterol by 63 amphipaths. *Biochemistry* 48, 8505-8515.
- (55) Ohno-Iwashita, Y., Iwamoto, M., Mitsui, K.-i., Ando, S., and Iwashita, S. (1991) A cytolysin, θ -toxin, preferentially binds to membrane cholesterol surrounded by phospholipids with 18-carbon hydrocarbon chains in cholesterol-rich region. *J. Biochem.(Tokyo)* 110, 369-375.
- (56) Zitzer, A., Bittman, R., Verbicky, C. A., Erukulla, R. K., Bhakdi, S., Weis, S., Valeva, A., and Palmer, M. (2001) Coupling of cholesterol and cone-shaped lipids in bilayers augments membrane permeabilization by the cholesterol-specific toxins streptolysin O and *Vibrio cholerae* cytolysin. *J. Biol. Chem.* 276, 14628-14633.
- (57) Clarke, J., and Fersht, A. R. (1993) Engineered disulfide bonds as probes of the folding pathway of barnase: Increasing the stability of proteins against the rate of denaturation. *Biochemistry* 32, 4322-4329.
- (58) Goni, F. M., and Alonso, A. (2000) Membrane fusion induced by phospholipase C and sphingomyelinases. *Biosci. Rep.* 20, 443-463.
- (59) Nieva, J. L., Goni, F. M., and Alonso, A. (1989) Liposome fusion catalytically induced by phospholipase C. *Biochemistry* 28, 7364-7367.
- (60) Takahashi, T., Sugahara, T., and Ohsaka, A. (1981) Phospholipase C from *Clostridium perfringens*. *Methods Enzymol.* 7, 710-725.
- (61) Palmer, M. (2004) Cholesterol and the activity of bacterial toxins. *FEMS Microbiol. Lett.* 238, 281-289.
- (62) Alouf, J. E., Billington, S. J., and Jost, B. H. (2006) Repertoire and general features of the family of cholesterol-dependent cytolysins, in *The comprehensive sourcebook of*

- 1
2
3 *bacterial protein toxins* (Alouf, J. E., and Popoff, M. R., Eds.) pp 643-658, Academic
4 Press, Oxford, England.
5
6
7
8 (63) Ohno-Iwashita, Y., Iwamoto, M., Ando, S., and Iwashita, S. (1992) Effect of lipidic
9 factors on membrane cholesterol topology - mode of binding of θ -toxin to cholesterol in
10 liposomes. *Biochim. Biophys. Acta* 1109, 81-90.
11
12
13
14
15 (64) Lange, Y., Ye, J., and Steck, T. L. (2005) Activation of membrane cholesterol by
16 displacement from phospholipids. *J. Biol. Chem.* 280, 36126-36131.
17
18
19
20 (65) Alving, C. R., Habig, W. H., Urban, K. A., and Hardegree, M. C. (1979) Cholesterol-
21 dependent tetanolysin damage to liposomes. *Biochim. Biophys. Acta* 551, 224-228.
22
23
24
25 (66) Rosenqvist, E., Michaelsen, T. E., and Vistnes, A. I. (1980) Effect of streptolysin O and
26 digitonin on egg lecithin/cholesterol vesicles. *Biochim. Biophys. Acta* 600, 91-102.
27
28
29
30 (67) Bavdek, A., Gekara, N. O., Priselac, D., Gutierrez Aguirre, I., Darji, A., Chakraborty, T.,
31 MacÍEek, P., Lakey, J. H., Weiss, S., and Anderluh, G. (2007) Sterol and pH
32 interdependence in the binding, oligomerization, and pore formation of listeriolysin O.
33
34 *Biochemistry* 46, 4425-4437.
35
36
37
38
39 (68) Hotze, E. M., Heuck, A. P., Czajkowsky, D. M., Shao, Z., Johnson, A. E., and Tweten, R.
40 K. (2002) Monomer-monomer interactions drive the prepore to pore conversion of a beta
41 -barrel-forming cholesterol-dependent cytolysin. *J. Biol. Chem.* 277, 11597-11605.
42
43
44
45
46 (69) Yeagle, P. L., and Young, J. E. (1986) Factors contributing to the distribution of
47 cholesterol among phospholipid vesicles. *J. Biol. Chem.* 261, 8175-8181.
48
49
50
51 (70) Veatch, S. L., and Keller, S. L. (2005) Miscibility phase diagrams of giant vesicles
52 containing sphingomyelin. *Phys. Rev. Lett.* 94, 148101-148104.
53
54
55
56
57
58
59
60

- 1
2
3
4 (71) Ziblat, R., Leiserowitz, L., and Addadi, L. Crystalline domain structure and cholesterol
5 crystal nucleation in single hydrated DPPC:Cholesterol:Popc bilayers. *J. Amer. Chem.*
6 *Soc. 132*, 9920-9927.
7
8
9
10 (72) Jacobs, T., Cima-Cabal, M. D., Darji, A., Méndez, F. J., Vázquez, F., Jacobs, A. A. C.,
11 Shimada, Y., Ohno-Iwashita, Y., Weiss, S., and de los Toyos, J. R. (1999) The conserved
12 undecapeptide shared by thiol-activated cytolysins is involved in membrane binding.
13 *FEBS Letters 459*, 463-466.
14
15
16
17 (73) Polekhina, G., Feil, S. C., Tang, J., Rossjohn, J., Giddings, K. S., Tweten, R. K., and
18 Parker, M. W. (2006) Comparative three-dimensional structure of cholesterol-dependent
19 cytolysins, in *The comprehensive sourcebook of bacterial protein toxins* (Alouf, J. E.,
20 and Popoff, M. R., Eds.) pp 659-670, Academic Press, Oxford, England.
21
22
23
24 (74) Pinkney, M., Beachey, E., and Kehoe, M. (1989) The thiol-activated toxin streptolysin o
25 does not require a thiol group for cytolytic activity. *Infect. Immun. 57*, 2553-2558.
26
27
28
29 (75) Saunders, F. K., Mitchell, T. J., Walker, J. A., Andrew, P. W., and Boulnois, G. J. (1989)
30 Pneumolysin, the thiol-activated toxin of *streptococcus pneumoniae*, does not require a
31 thiol group for in vitro activity. *Infect. Immun. 57*, 2547-2552.
32
33
34
35 (76) Korchev, Y. E., Bashford, C. L., Pederzolli, C., Pasternak, C. A., Morgan, P. J., Andrew,
36 P. W., and Mitchell, T. J. (1998) A conserved tryptophan in pneumolysin is a determinant
37 of the characteristics of channels formed pneumolysin in cells and planar lipid bilayers.
38 *Biochem. J. 329*, 571-577.
39
40
41
42 (77) Michel, E., Reich, K. A., Favier, R., Berche, P., and Cossart, P. (1990) Attenuated
43 mutants of the intracellular bacterium *listeria monocytogenes* obtained by single amino
44 acid substitutions in listeriolysin o. *Molec. Microbiol. 4*, 2167-2178.
45
46
47
48
49
50
51
52
53
54
55
56
57
58
59
60

- 1
2
3 (78) Stachowiak, R., Wisniewski, J., Osinska, O., and Bielecki, J. (2009) Contribution of
4 cysteine residue to the properties of *Listeria monocytogenes* listeriolysin O. *Can. J.*
5
6 *Microbiol.* 55, 1153-1159.
7
8
9
10 (79) Cooper, R. A., Leslie, M. H., Fischkoff, S., Shinitzky, M., and Shattil, S. J. (1978)
11
12 Factors influencing the lipid composition and fluidity of red cell membranes in vitro:
13
14 Production of red cells possessing more than two cholesterols per phospholipid.
15
16 *Biochemistry* 17, 327-331.
17
18
19
20 (80) Jacobs, T., Darji, A., Frahm, N., Rohde, M., Wehland, J., Chakraborty, T., and Weiss, S.
21
22 (1998) Listeriolysin O: Cholesterol inhibits cytolysis but not binding to cellular
23
24 membranes. *Molec. Microbiol.* 28, 1081-1089.
25
26
27 (81) Gaus, K., Rodriguez, M., Ruberu, K. R., Gelissen, I., Sloane, T. M., Kritharides, L., and
28
29 Jessup, W. (2005) Domain-specific lipid distribution in macrophage plasma membranes.
30
31 *J. Lipid Res.* 46, 1526-1538.
32
33
34 (82) Harwood, C. R., and Cranenburgh, R. (2008) *Bacillus* protein secretion: An unfolding
35
36 story. *Trends Microbiol.* 16, 73-79.
37
38
39 (83) Rafii, F., Park, M., Bryant, A. E., Johnson, S. J., and Wagner, R. D. (2007) Enhanced
40
41 production of phospholipase C and perfringolysin O (alpha and theta toxins) in a
42
43 gatifloxacin-resistant strain of *Clostridium perfringens*. *Antimicrob. Agents Chemother.*,
44
45 52, 895-900.
46
47
48 (84) Hamman, B. D., Hendershot, L. M., and Johnson, A. E. (1998) BiP maintains the
49
50 permeability barrier of the ER membrane by sealing the luminal end of the translocon
51
52 pore before and early in translocation. *Cell* 92, 747-758.
53
54
55
56
57
58
59
60

- 1
2
3
4
5
6
7
8
9
10
11
12
13
14
15
16
17
18
19
20
21
22
23
24
25
26
27
28
29
30
31
32
33
34
35
36
37
38
39
40
41
42
43
44
45
46
47
48
49
50
51
52
53
54
55
56
57
58
59
60
- (85) Urbina, P., Flores-Díaz, M., Alape-Girón, A., Alonso, A., and Goni, F. M. (2009) Phospholipase C and sphingomyelinase activities of the *Clostridium perfringens* α -toxin. *Chem. Phys. Lip.* 159, 51-57.
- (86) Goldfine, H., Knob, C., Alford, D., and Bentz, J. (1995) Membrane permeabilization by *Listeria monocytogenes* phosphatidylinositol-specific phospholipase C is independent of phospholipid hydrolysis and cooperative with listeriolysin O. *Proc. Natl. Acad. Sci. U. S. A.* 92, 2979-2983.
- (87) Smith, G. A., Marquis, H., Jones, S., Johnston, N. C., Portnoy, D. A., and Goldfine, H. (1995) The two distinct phospholipases C of *Listeria monocytogenes* have overlapping roles in escape from a vacuole and cell-to-cell spread. *Infect. Immun.* 63, 4231-4237.
- (88) Birmingham, C. L., Canadien, V., Kaniuk, N. A., Steinberg, B. E., Higgins, D. E., and Brumell, J. H. (2008) Listeriolysin O allows *Listeria monocytogenes* replication in macrophage vacuoles. *Nature* 451, 350-354.
- (89) Alberti-Segui, C., Goeden, K. R., and Higgins, D. E. (2007) Differential function of *Listeria monocytogenes* listeriolysin O and phospholipases C in vacuolar dissolution following cell-to-cell spread. *Cell. Microbiol.* 9, 179-195.
- (90) Barlic, A., Gutierrez-Aguirre, I., Caaveiro, J. M., Cruz, A., Ruiz-Arguello, M. B., Perez-Gil, J., and Gonzalez-Manas, J. M. (2004) Lipid phase coexistence favors membrane insertion of equinatoxin-II, a pore-forming toxin from *Actinia equina*. *J. Biol. Chem.* 279, 34209-34216.

TABLES

TABLE 1. Fluorescence emission maxima and relative total fluorescence intensity for commonly used PFO derivatives. The emission fluorescence maxima and relative total intensity is indicated for total aromatic amino acids ($\lambda_{\text{ex}} = 270$ nm) or selectively for the Trp residues ($\lambda_{\text{ex}} = 297$ nm). Emission scans were performed and corrected as described in experimental procedures. Total intensities were obtained from the area under the curve for the corrected spectra. The average and range for two independent determinations is shown.

Derivative	$\lambda_{\text{ex}} = 270$ nm		$\lambda_{\text{ex}} = 297$ nm	
	λ_{em} max	Relative Total	λ_{em} max	Relative Total
		Intensity		Intensity
nPFO	321.5 \pm 0.5	1.00	330.5 \pm 0.5	1.0
rPFO	328.5 \pm 0.5	1.62 \pm 0.04	333.5 \pm 0.5	2.0 \pm 0.1
pAH21His	328.5 \pm 0.5	1.62 \pm 0.02	333.0 \pm 0.5	2.1 \pm 0.1
pRT20	332.5 \pm 0.5	1.87 \pm 0.03	336.0 \pm 0.5	2.4 \pm 0.2

FIGURE LEGENDS

1
2
3
4
5
6
7
8
9
10
11
12
13
14
15
16
17
18
19
20
21
22
23
24
25
26
27
28
29
30
31
32

Fig. 1. **Cholesterol dependence of nPFO binding to membranes composed of cholesterol and glycerolipids with different head groups.** nPFO binding to liposomal membranes was followed by the increase in the net Trp emission intensity ($F_{\text{memb}}/ F_{\text{sol}}$) calculated as described in experimental procedures. **A)** Binding of nPFO to POPC/cholesterol liposomes (filled circles). The mol% of cholesterol was increased from 25% to 55%. **B)** Binding of nPFO to membranes containing a constant 35 mol% cholesterol and different ratios of POPE/POPC, ranging from 0 (no POPE) to 1.9; (open circles). **C)** Binding of nPFO to membranes containing 35 mol% cholesterol and different ratios of DAG/POPC ranging from 0 (no DAG) to 1; (open circles). In all panels, pore formation was evaluated using liposomes prepared with selected lipid compositions, and the fraction of fluorophore quenched is indicated using bars. Each data point shows the average of at least two independent measurements and their range.

33
34
35
36
37
38
39
40
41
42
43
44
45
46
47
48
49
50
51
52
53
54
55
56
57
58
59
60

Fig. 2. **Cholesterol dependent binding and stability of nPFO and rPFO.** **A)** The fraction of bound rPFO (open circles) is compared with the fraction of bound nPFO (filled circles) to POPC liposomes containing the indicated amount of cholesterol. Measurements were done as indicated in Fig. 1, and normalized to account for the difference in the total fluorescence observed for each mutant. **B)** Urea denaturation and renaturation of nPFO. The average energy of emission for each fluorescence emission spectrum was obtained for nPFO at given urea concentrations. Samples of nPFO in buffer A or nPFO in urea 6M in buffer A, were added and equilibrated at the indicated urea concentration as described in experimental procedures. **C)** Urea denaturation for rPFO and nPFO. The average energy of emission for each fluorescence emission spectrum was obtained for nPFO or rPFO at given urea concentrations. The data in B) and C) were fitted assuming that

1
2
3 the average energy of emission of the folded and unfolded states varies linearly with urea
4 concentration.
5
6

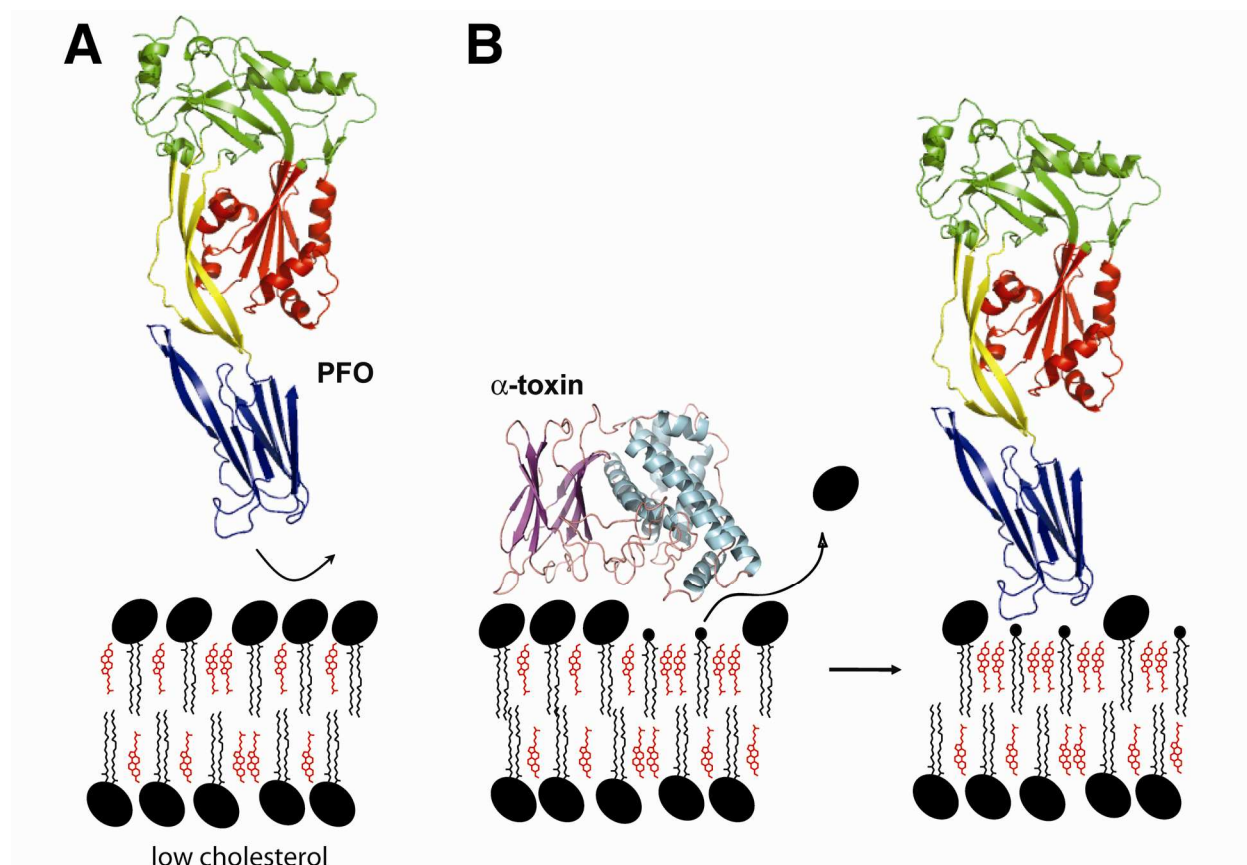
7
8 **Fig. 3. *C. perfringens* α -toxin action facilitates PFO-membrane binding and pore formation.**

9
10 Kinetic profiles for the pore-formation activity of nPFO (panels A, C, E, G) or rPFO (panels B,
11 D, F) on POPC liposomes containing the indicated amount of cholesterol (mol% of total lipids).
12 Pore formation was determined by the quenching of a liposome-encapsulated GSH-Fl by the
13 externally added anti-Fl antibody as detailed in experimental procedures. Liposomes were
14 incubated at 37°C either with 0.5 units/ml of α -toxin (open circles) or without (control, filled
15 circles) for 15 min whereupon PFO protein was added to a final concentration of 300 nM.
16 Typical error ranges obtained for two independent measurements are shown in panel C. A
17 typical profile for GSH-Fl quenching on liposomes incubated with α -toxin but without addition
18 of PFO is shown in panel E (control). The time of addition of α -toxin and PFO (or equivalent
19 buffer solutions) at 0 min and 15 min, respectively, are indicated by the arrows at the top of the
20 panels.
21
22
23
24
25
26
27
28
29
30
31
32
33
34
35
36
37

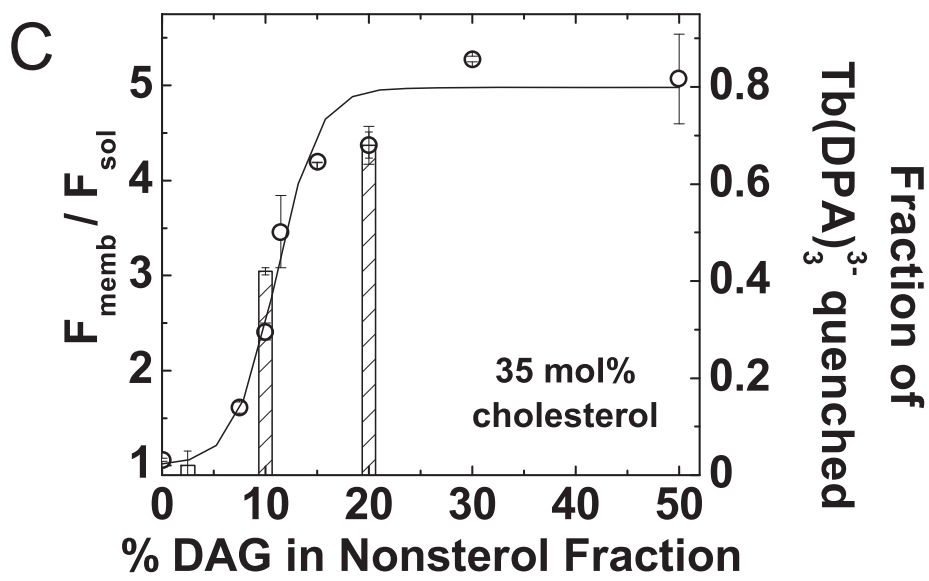
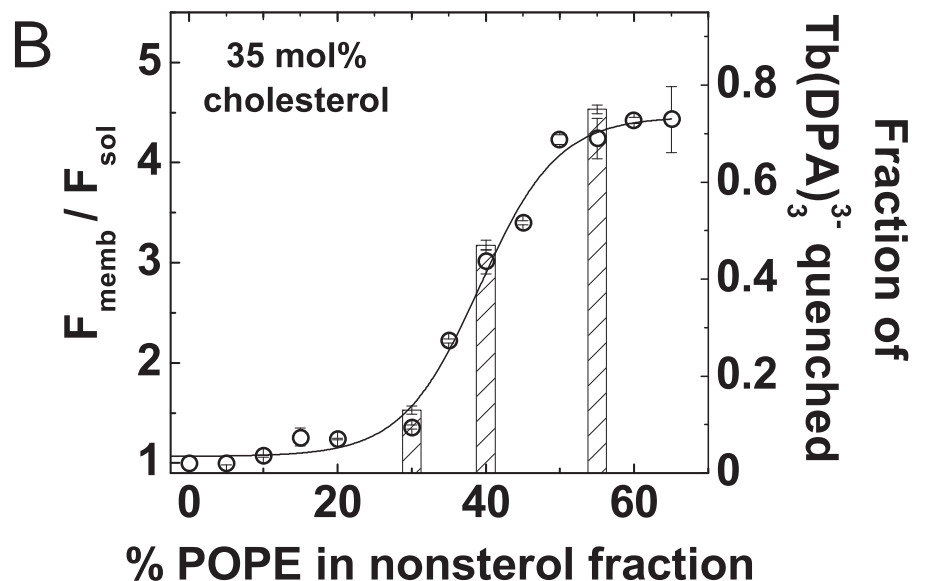
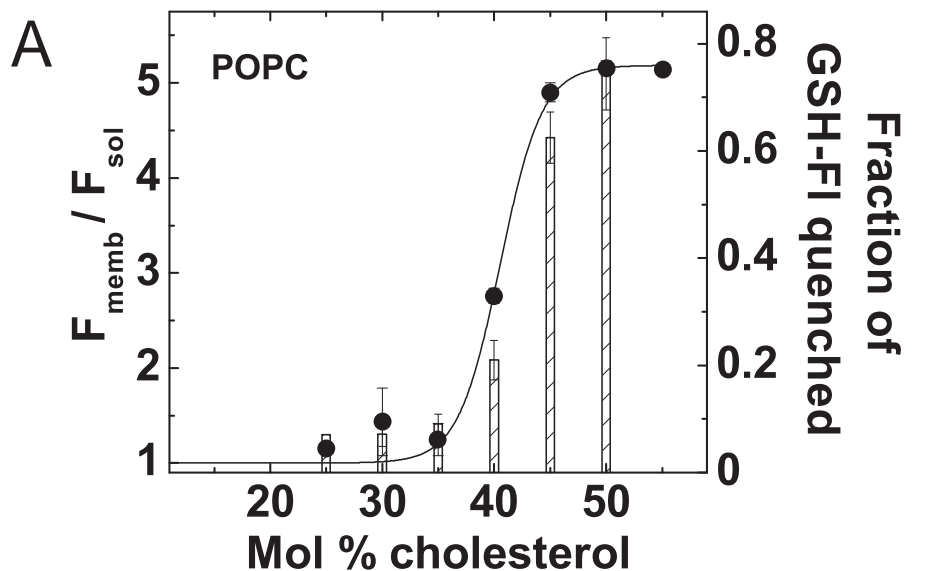
38 **Fig. 4. A schematic model for the *C. perfringens* α -toxin effect on PFO binding.**

39 A) PFO
40 does not bind to membranes containing low cholesterol content, presumably because no free
41 cholesterol molecules are present in the membrane. B) *C. perfringens* α -toxin hydrolyzes PC
42 releasing the phosphocholine head-group and generating DAG. The appearance of free
43 cholesterol molecules triggers D4-mediated PFO binding. PFO and α -toxin cartoon
44 representations were generated using PyMol (Delano Scientific). The phosphocholine head-
45 group of POPC is represented as a large black oval. The glycerol moiety of DAG is shown as a
46 small black circle.
47
48
49
50
51
52
53
54
55
56
57
58
59
60

Graphic image to represent the paper within the Table of Contents



1
2
3
4
5
6
7
8
9
10
11
12
13
14
15
16
17
18
19
20
21
22
23
24
25
26
27
28
29
30
31
32
33
34
35
36
37
38
39
40
41
42
43
44
45
46
47
48
49
50
51
52
53
54
55
56
57
58
59
60



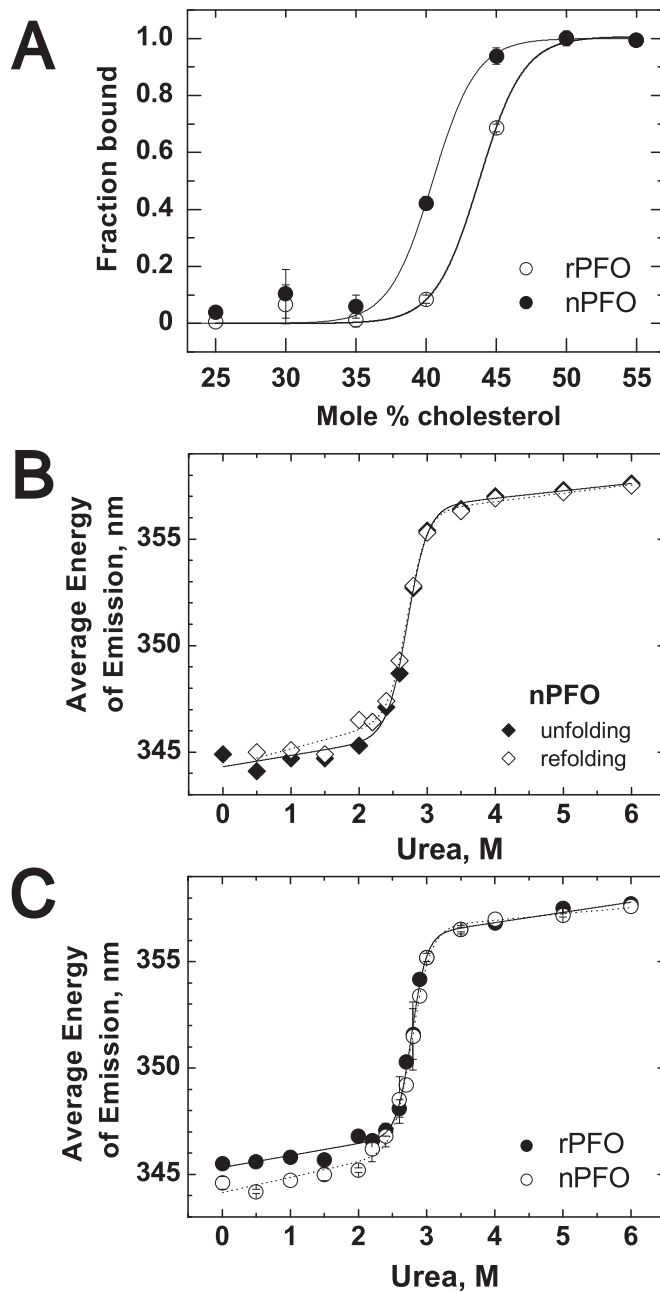
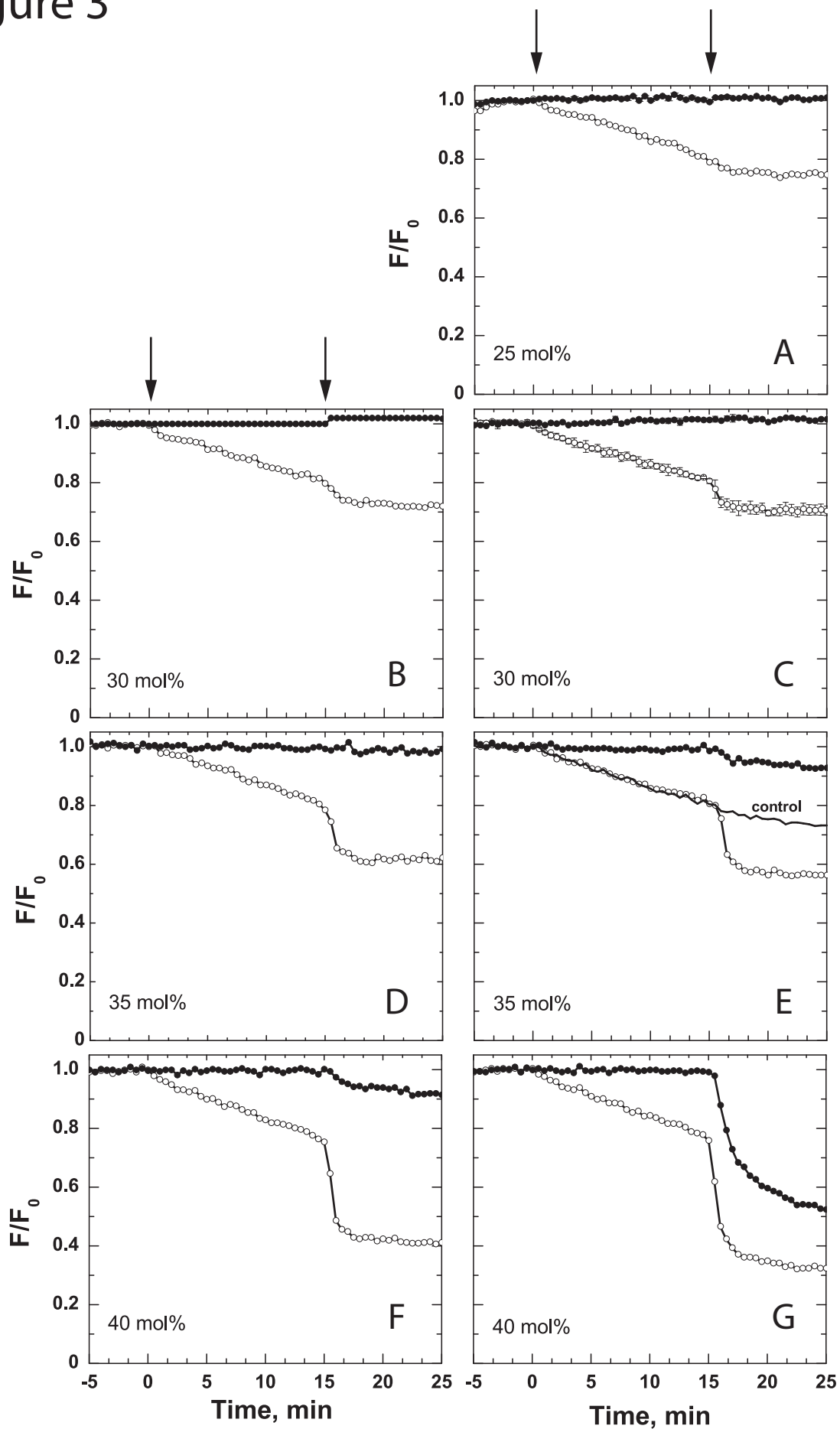
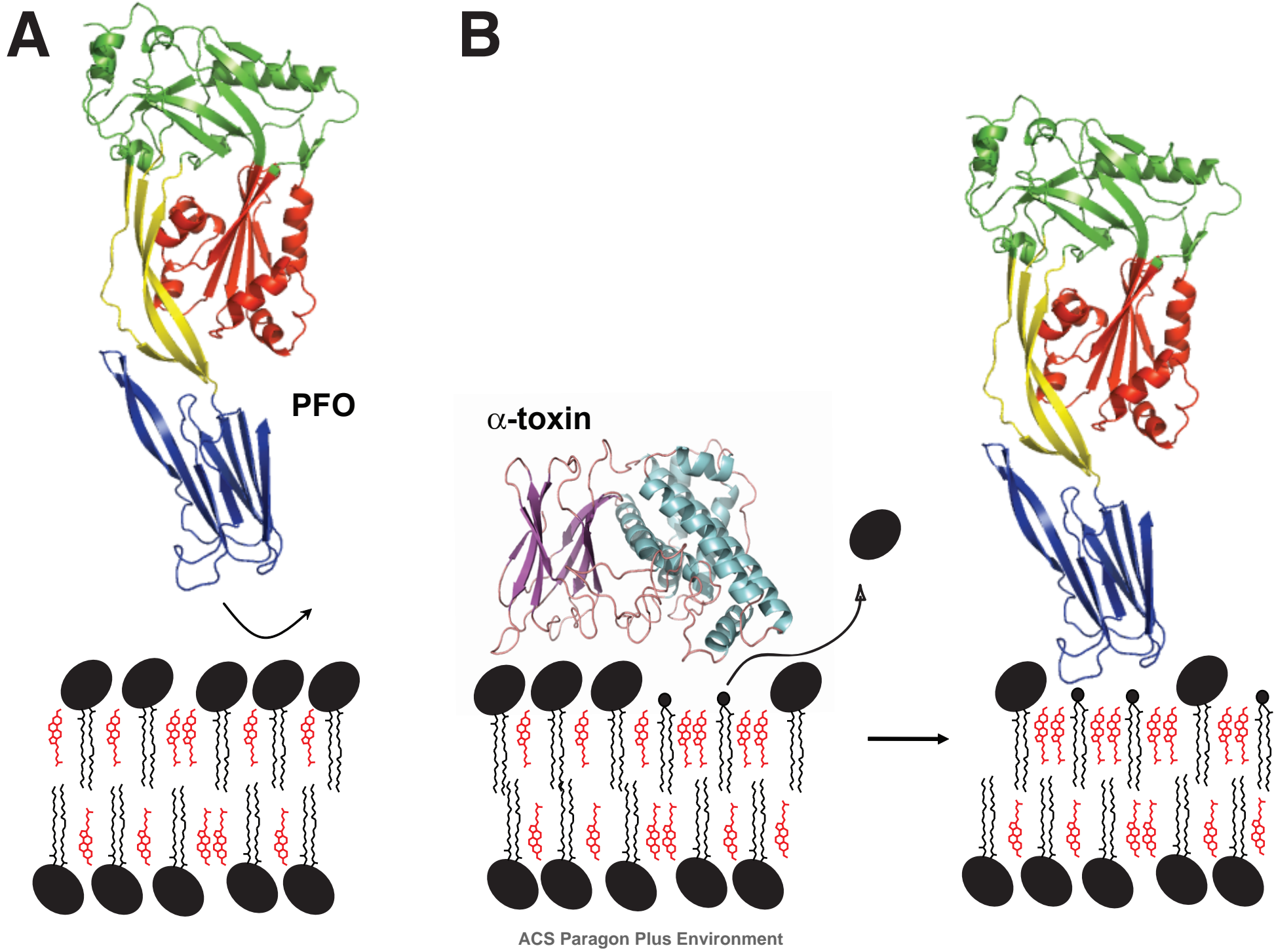


Figure 3





1
 2
 3
 4
 5
 6
 7
 8
 9
 10
 11
 12
 13
 14
 15
 16
 17
 18
 19
 20
 21
 22
 23
 24
 25
 26
 27
 28
 29
 30
 31
 32
 33
 34
 35
 36
 37
 38
 39
 40
 41
 42
 43
 44
 45
 46
 47
 48
 49